Thymus-homing peripheral dendritic cells constitute two of the three major subsets of dendritic cells in the steady-state thymus

JiChu Li,[1] JooHung Park,[2] Deborah Foss,[3] and Irving Goldschneider[3]

[1]Department of Viral Pathogenesis, Beth Israel Deaconess Medical Center, Boston, MA 02215
[2]Department of Biology, Changwon National University, Changwon, Kyongnam, 641-773, Korea
[3]Department of Immunology, School of Medicine, University of Connecticut Health Center, Farmington, CT 06030

Many dendritic cells (DCs) in the normal mouse thymus are generated intrathymically from common T cell/DC progenitors. However, our previous work suggested that at least 50% of thymic DCs originate independently of these progenitors. We now formally demonstrate by parabiotic, adoptive transfer, and developmental studies that two of the three major subsets of thymic DCs originate extrathymically and continually migrate to the thymus, where they occupy a finite number of microenvironmental niches. The thymus-homing DCs consisted of immature plasmacytoid DCs (pDCs) and the signal regulatory protein α–positive (Sirpα$^+$) CD11b$^+$ CD8α$^-$ subset of conventional DCs (cDCs), both of which could take up and transport circulating antigen to the thymus. The cDCs of intrathymic origin were mostly Sirpα$^-$ CD11b$^-$ CD8α^{hi} cells. Upon arrival in the thymus, the migrant pDCs enlarged and up-regulated CD11c, major histocompatibility complex II (MHC II), and CD8α, but maintained their plasmacytoid morphology. In contrast, the migrant cDCs proliferated extensively, up-regulated CD11c, MHC II, and CD86, and expressed dendritic processes. The possible functional implications of these findings are discussed.

CORRESPONDENCE
Irving Goldschneider:
igoldsch@neuron.uchc.edu

Abbreviations used: 7-AAD, 7-aminoactinomycin D; cDC, conventional DC; CSA, cyclosporin A; eGFP, enhanced GFP; pDC, plasmacytoid DC; Sirpα, signal regulatory protein α; tg, transgenic.

Three major subsets of DCs have been identified in the mouse and human thymus (1). The most intensively studied subset in the mouse has a signal regulatory protein α–negative (Sirpα$^-$) CD11b$^-$ CD8α^{hi} phenotype and is thought to arise intrathymically from a common T cell/DC precursor. These conventional DCs (cDCs) are generally presumed to be involved in the negative selection of developing thymocytes. In contrast, the origins and in vivo functions of the two other subsets of thymic DCs are unknown. One subset is composed of plasmacytoid DCs (pDCs) and the other is composed of Sirpα$^+$ CD11b$^+$ CD8α$^-$ cDCs.

In previous parabiotic and adoptive transfer experiments, we provided evidence that at least 50% of the DCs in the steady-state thymus developed independently of thymocyte progenitors (2). These included pDCs and possibly the subset of CD11b$^+$ CD8α$^-$ cDCs. In contrast, most of the DCs whose generation was linked to the importation of thymocyte progenitors were CD11b$^-$ CD8α^{hi} cDCs, as also suggested by the experiments of Porritt et al. (3). These results raised the possibility that two of the three subsets of thymic DCs might be formed extrathymically.

In studies involving the induction of immune deviation (Th1 to Th2 polarization) in mice injected intraocularly with antigen, we detected a population of F4/80$^+$ antigen-presenting cells that migrated to the thymus and activated NKT reg cells (unpublished data) (4, 5). We also observed that self–MHC II–specific CD4$^+$ CD25$^+$ T reg cells appeared in the thymus of post–cyclosporin A (CSA)–treated mice at the time when an influx of tolerogenic DCs from the periphery occurs (6–8). In addition, abundant evidence from other laboratories has demonstrated that thymus-homing inflammatory DCs can induce both dominant and deletional tolerance to peripheral self- and nonself-antigens (see Discussion). These observations led us to hypothesize that, in addition to the promiscuous intrathymic expression of tissue-restricted antigens (9), the migration of

The Rockefeller University Press $30.00
J. Exp. Med. Vol. 206 No. 3 607-622
www.jem.org/cgi/doi/10.1084/jem.20082232

The Journal of Experimental Medicine

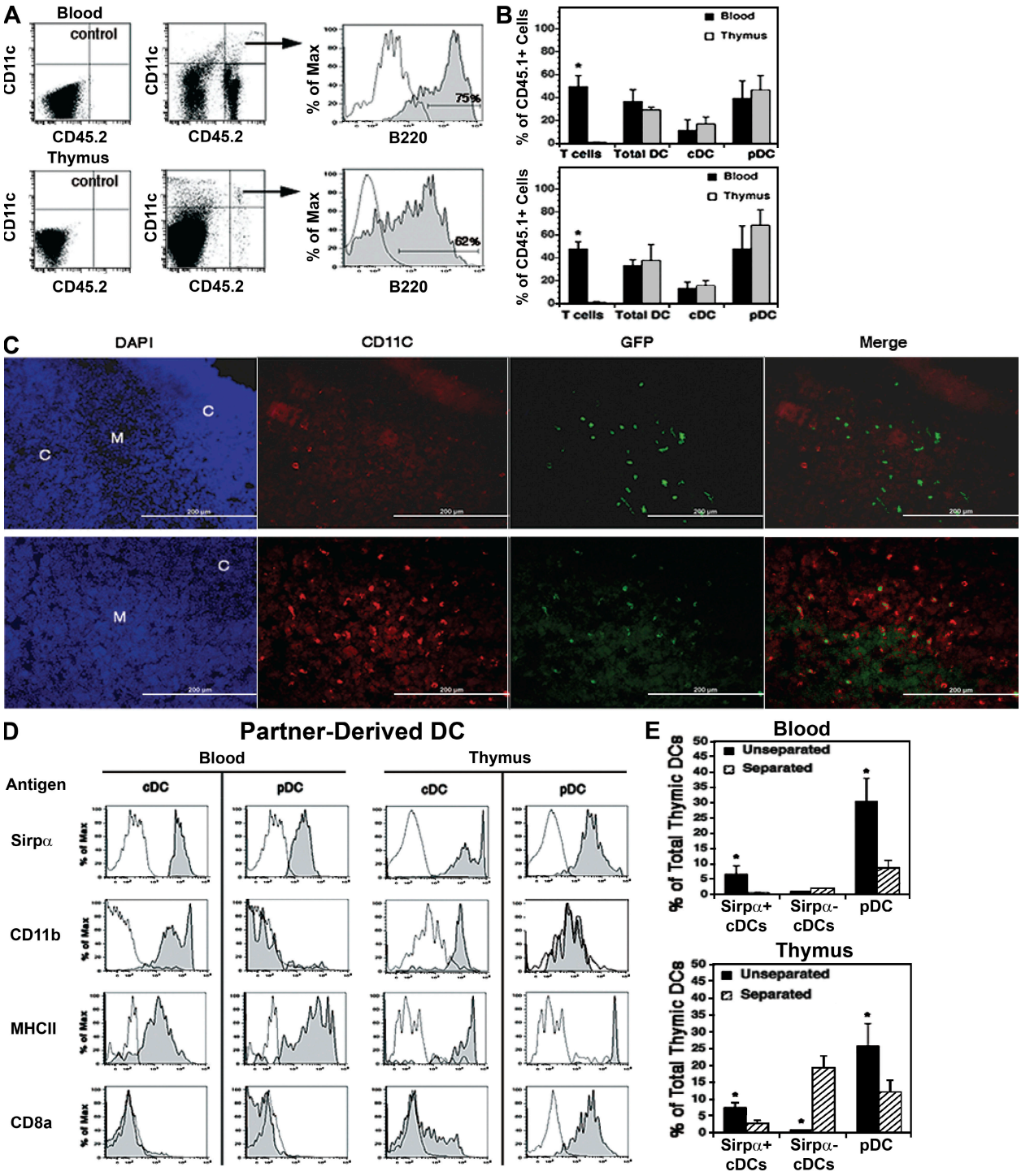

Figure 1. Partner-derived DCs in the blood and thymus of parabiotic mice. CD45.1 and CD45.2 congenic mice or eGFP tg and WT mice were joined by cutaneous vascular anastomosis. (A–D) The blood and thymus of each partner were harvested at week 3. (E) The parabiotic mice were separated at week 3 and rested for 4 wk before harvest of the blood and thymus. Five-color FACS analysis for CD45.1, CD45.2, or GFP plus CD11c, B220, Sirpα, and one of the other surface antigens listed in D was performed on each sample. Background fluorescence (unshaded profiles) was determined by omitting only the relevant antibody. (A) Partner-derived DCs ($CD45.2^+$ $CD11c^+$ in this example) were identified in the blood and thymus (arrows), and the percentages of cDCs and pDCs (shaded profiles) were determined by analysis for $B220^-$ and $B220^+$ cells, respectively. Note that numerous $CD11c^-$ donor-origin cells (mostly $CD3^+$ T cells) were present in the blood but not the thymus. A representative analysis is shown (1 out of 16 parabiotic partners from two experiments). (B) Percentage of each indicated cell population in the blood and thymus that was partner derived. Data are means ± SD of four parabiotic pairs from one out of two experiments. *, $P < 0.05$ between paired values for the blood and thymus. (C) Location of partner-derived DCs (GFP^+ $CD11c^+$) in the thymus by immunohistology. (top) Isotype controls for CD11c examined by three-color fluorescence microscopy of the same field for DAPI (blue), GFP

DCs from the blood to thymus constituted a major pathway by which the induction of dominant and deletional thymic tolerance to peripheral self- and nonself-antigens may also occur under steady-state conditions (2, 10).

Although the present study does not formally test this hypothesis, it does provide supporting data by demonstrating that (a) most, if not all, of the pDCs and approximately one third of the cDCs (those expressing Sirpα and CD11b) in the steady-state thymus are recent emigrants from the blood; (b) immature, noninflammatory, thymus-homing pDCs and cDCs can take up both soluble and particulate circulating antigen and transport it to the thymus; (c) once in the thymus, the pDCs enlarge and assume a semimature phenotype by up-regulating CD11c, MHC II, and CD8α (but not CD86) while maintaining a plasmacytoid morphology; and (d) the thymus-homing Sirpα$^+$ CD11b$^+$ cDCs proliferate extensively in the thymus, up-regulate CD86 as well as CD11c and MHC II, and assume a mature DC morphology. Some of the functional implications of these findings have recently been reported by Proietto et al. (11), who observed that the Sirpα$^+$ CD11b$^+$ subset of thymic cDCs could induce CD4$^+$ CD25$^+$ Foxp3$^+$ T reg cells from CD4$^+$ CD25$^-$ Foxp3$^-$ thymocytes in vitro, and that thymus-homing DCs could induce antigen-specific (OVA) deletion and T reg cell formation in transplanted thymus lobes in vivo. Given the propensity of semimature pDCs to induce T reg cells in the periphery (12–14), it is possible that they too may contribute to the induction of central tolerance.

RESULTS

Migration of DCs to the thymus in parabiotic mice

Our previous experiments suggested that 50% of the total DCs present in the thymi of adult mice arise independently of thymocyte progenitors and may have emigrated in a preformed state from the blood (2). In this study, we set up pairs of parabiotic mice between CD45.1 and CD45.2 partners to confirm this hypothesis and to determine the phenotypes and origins of the partner-derived thymic DCs. In these experiments, partner-derived pDCs and cDCs in the blood and thymus were examined 3 wk after parabiotic union, when thymocyte chimerism was still very low (Fig. 1 A). Because T cells are exchanged randomly in the blood of parabiotic partners but few migrate to the thymus (15), we used them as a standard against which to judge the efficiency of cross-transfer and thymic migration of hematogenous DCs.

As shown in Fig. 1 B, pDCs, like T cells, were randomly exchanged in the blood of the parabiotic pairs, whereas only ∼12% of the total cDCs were exchanged. This suggested that most pDCs recirculate in the blood but that most cDCs do not. Similarly, ∼50% of the pDCs and 15% of the cDCs in each thymus were partner derived. Given that ∼30% of the total DCs in the thymus were pDCs and 70% were cDCs, it can be calculated that partner-derived DCs comprised ∼25% of the total DCs in each thymus (0.5 × 30% pDCs + 0.15 × 70% cDCs). By doubling these figures to allow for an equivalent contribution by thymus-homing host-origin DCs, we estimate that ∼50% of the total DCs in each thymus (i.e., most if not all of the pDCs and about one third of the cDCs) had been formed extrathymically and/or had originated from committed thymus-homing precursors. As shown by immunohistology (Fig. 1 C), most of the partner-derived DCs (GFP$^+$ in this case) were comingled with the host-origin DCs in the thymus medulla and corticomedullary regions.

These results clearly indicated that the partner-derived pDCs had migrated randomly from the blood to thymus and reached equilibrium within 3 wk. However, as the partner-derived cDCs constituted <15% of the total cDCs in the blood and thymus, it was not possible to deduce whether they too had reached equilibrium. To do this, it first was necessary to distinguish the thymus-homing cDC subset from other cDCs in the blood and thymus. As shown in Fig. 1 D, almost all of the partner-derived cDCs in the blood and thymus were Sirpα$^+$ CD11b$^+$ MHC II$^+$, and ∼20% of those in the thymus were CD8α$^{lo/int}$. In contrast, the major subset of host-derived cDCs in the blood and thymus were Sirpα$^-$ CD11b$^-$ MHC II$^+$, and almost all of those in the thymus were CD8α^{hi} (unpublished data). As with the pDCs, ∼50% of the total Sirpα$^+$ CD11b$^+$ cDCs in both the blood and thymus were partner derived. Therefore, it can be deduced that the partner-derived cDCs also equilibrated between the blood and thymus within 3 wk of parabiotic union. However, as the partner-derived cDCs in the thymus expressed higher mean levels of Sirpα and MHC II (Fig. 1 D), they appeared to be more mature than those in the blood. Similarly, the partner-derived pDCs in the thymus expressed higher levels of MHC II, and almost all displayed CD8α (16, 17).

To confirm the intrathymic origin of the Sirpα$^-$ CD11b$^-$ CD8α^{hi} subset of thymic cDCs, mice were parabiosed for 3 wk, and then separated and rested for 4 wk. Our prediction, based

(green), and CD11c (red). (bottom) A comparable field stained for CD11c. The cortical (C) and medullary (M) regions are indicated in the DAPI-stained panels, the donor-origin cells are indicated by GFP fluorescence, and the total DCs are indicated by the CD11c staining. Representative sections from one out of three GFP$^-$ parabiotic partners are shown. Bars, 200 µm. (D) Surface phenotypes of partner-derived cDCs and pDCs in the blood and thymus were determined by FACS analysis for Sirpα, CD11b, MHC II, and/or CD8α (shaded profiles) as compared with background fluorescence (unshaded profiles). Representative analyses of parabiotic partners from one out of two experiments are shown. (E) Effects of interrupting the cross-exchange of blood on the levels of DC chimerism in the blood and thymus of parabiotic mice. Pairs of mice were sacrificed 3 wk after parabiosis (unseparated), or were surgically separated and rested for 4 wk before being sacrificed (separated). The relative percentage of total pDCs, Sirpα$^+$ CD11b$^+$ cDCs, and Sirpα$^-$ CD11b$^-$ cDCs of partner origin were determined by FACS analysis. Data are means ± SD of four pairs of parabiotic mice from one out of two experiments. Each bar represents the pooled results from four parabiotic partners. *, $P < 0.01$ between unseparated and separated mice.

on previous studies (2, 18), was that partner-derived thymocyte progenitors would enter the thymus at some point during the first 3 wk of parabiosis and would generate a wave of thymocytes and Sirpα$^-$ CD11b$^-$ CD8α$^+$ cDCs thereafter. However, because of the absence of significant bone marrow chimerism at this time, the partner-derived pDCs and Sirpα$^+$ CD11b$^+$ cDCs in the blood would not be replenished during the month of separation. The results in Fig. 1 E are compatible with this scenario.

Migration of DCs to the thymus after adoptive transfer

Collectively, the results in the parabiotic mice suggested that small numbers of pDCs and Sirpα$^+$ CD11b$^+$ cDCs continuously enter the steady-state thymus from the blood. To test this prediction, nonirradiated WT mice were injected i.v. with 20 × 10^6 nucleated blood cells from enhanced GFP (eGFP) transgenic (tg) mice, a cell dose that contained approximately the same number and variety of DCs as are normally present in the blood (~2.5 ml) of an adult mouse. At timed

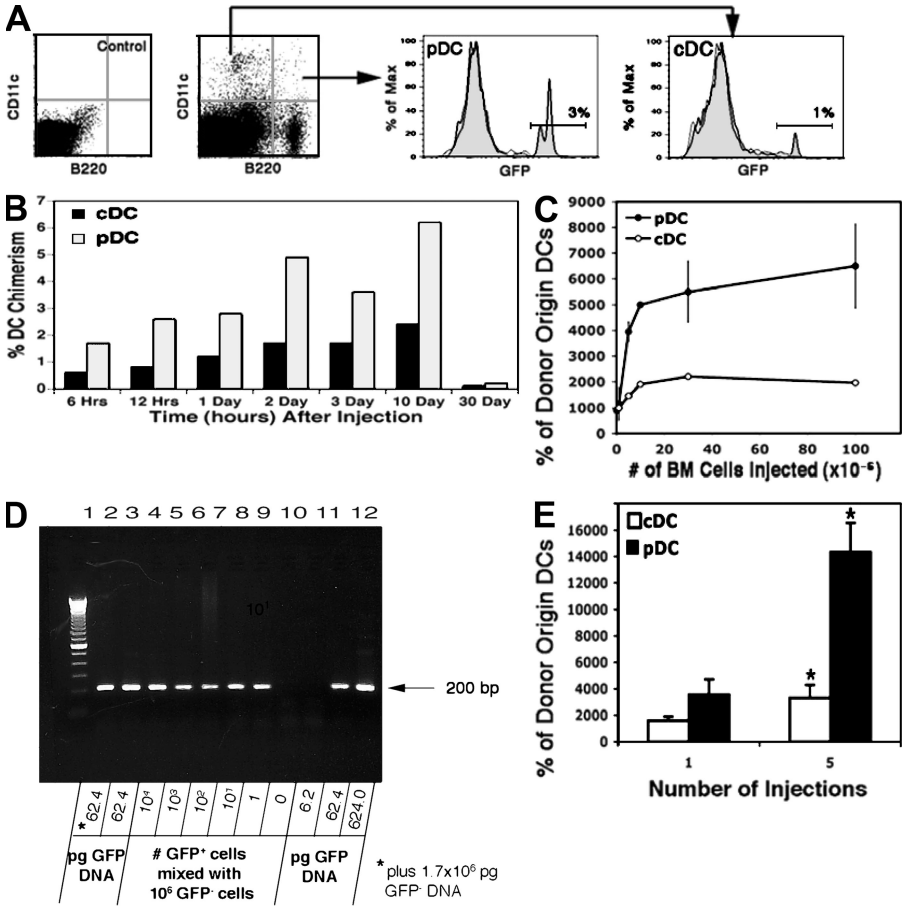

Figure 2. Migration of DCs to the thymus of normal adoptive recipients. (A) 20 million nucleated blood cells from adult eGFP tg mice were injected i.v. into 5–7-wk-old nonirradiated WT recipients. Thymus cells were harvested 2 d later, total cDCs and pDCs were identified (arrows), and the percentage that were of donor origin (GFP$^+$) was determined. Thymic cDCs and pDCs from GFP$^{-/-}$ control mice were used to determine background fluorescence. More than 90% of the B220$^+$ donor-origin cells were PDCA$^+$ Gr-1$^+$ NK1.1$^-$, and >90% of the B220$^-$ donor-origin cells were PDCA$^-$ Gr-1$^-$ NK1.1$^-$ (Fig. 3). Density gradient–enriched (40–50%) DCs from adoptive recipients showed comparable results. A representative analysis from >60 mice in eight experiments is shown. (B) Time–response. WT mice were injected i.v. with 20 × 10^6 bone marrow cells from eGFP tg mice, the thymocytes were harvested at the indicated times thereafter, and the percentage of the total cDCs and pDCs that were of donor origin (GFP$^+$) were determined. A representative analysis from one out of three experiments is shown. (C) Dose–response. The total numbers of donor-origin (GFP$^+$) pDCs and cDCs in the recipient thymus were determined 2 d after i.v. injection of graded numbers of bone marrow cells from eGFP tg mice, as indicated. Each point represents the mean ± SD of five recipients from one out of two experiments. (D) The sensitivity of the PCR assay was determined by serial dilution of thymic DNA from eGFP tg mice (lanes 10 to 12), and the numbers of cell equivalents were determined by dividing the pg of DNA by 6.24. Further resolution between 62.4 and 6.24 pg DNA revealed a sensitivity of two cell equivalents (not depicted). The sensitivity of the PCR assay was also determined by analyzing purposeful mixtures of GFP$^+$ thymic DCs and GFP$^-$ thymocytes (lanes 3–9) or a mixture of 62.4 pg GFP$^+$ DNA with 1.7 × 10^6 pg GFP$^-$ DNA (lanes 2 and 3). Lane 1 represents a 100-bp DNA ladder. A representative analysis from one out of eight experiments is shown. (E) Multiple injections. Groups of five normal WT mice were injected i.v. with either a single dose (20 × 10^6) of bone marrow cells from eGFP tg mice or five consecutive doses on alternate days. Thymocytes were harvested 2 d after the single dose or the last of the multiple doses, and the mean (±SD) total numbers of GFP$^+$ cDCs and pDCs per thymus were determined. *, $P < 0.01$ between the respective data for one and five injections. A representative analysis from one out of two experiments is shown.

intervals, the numbers and identities of the donor-origin DCs in the thymus were determined by FACS analysis (Fig. 2 A).

As shown in Fig. 2 B, donor-origin pDCs and cDCs entered the thymus as early as 6 h after i.v. transfer and increased progressively to reach a plateau at about day 2, at which time few donor-origin DCs were detectable in the blood. Both the donor-origin pDCs and cDCs persisted in the thymus for at least 10 d but were absent by 30 d. Results of multiple experiments showed that a mean of 4.5 ± 0.6% of the total pDCs and 0.9 ± 0.4% of the total cDCs were of donor origin at 2 d. As 30% of the total DCs in the thymus were pDCs and 70% were cDCs, it can be calculated that the ratio of donor-origin pDCs to cDCs in the thymus at this time was 2:1 (0.045 × 30% pDCs/0.009 × 70% cDCs). Similar results were obtained after i.v. injection of 20×10^6 lymph node, spleen, bone marrow, or thymus cells, even though the thymus cell suspensions contained ∼10% of the number of DCs as the others did (unpublished data).

Dose–response experiments (Fig. 2 C) demonstrated roughly parallel saturation kinetics for the donor-origin pDCs and cDCs 2 d after the injection of between 5 and 100×10^6 bone marrow cells. This suggested that the thymus has a finite number of niches for migrating DCs. Given the small number of donor-origin DCs present in the thymus 2 d after i.v. injection (∼8,000), we verified the results obtained by FACS analysis by nested PCR for GFP genomic DNA (Fig. 2 D). We also excluded the possibility that most of the donor-origin DCs were located in the blood passing through the thymus. As previously reported (19) and observed in this study, <1% of the injected DCs were present in heart blood after 2 d. Therefore, assuming a blood volume of 10% of organ weight, a maximum of only 18 GFP^+ cells could have been present in the ∼7 µl of thymus blood. The additional possibility that the donor-origin DCs were sequestered in the thymic blood vessels was excluded by examining immunohistological sections (unpublished data). Instead, as in the parabiotic mice (Fig. 1 C), almost all of the donor-origin DCs were located extravascularly in the medullary regions.

To gain some insight into relative turnover rates of thymus-homing pDCs and cDCs, mice were injected i.v. on alternate days with saturating doses of bone marrow cells for a total of five injections. As shown in Fig. 2 E, the number of donor-origin pDCs in the thymus 2 d after the fifth injection was four times greater than after the first injection. However, the number of donor-origin cDCs was only twofold greater. Hence, the turnover rate of the donor-origin DCs in the thymus appeared to approximate 12 d for the pDCs but only 3–4 d for the cDCs. These results are consistent with the equilibration rate for pDCs in the thymus (2), and with the reported life spans of pDCs and cDCs in the normal mouse spleen (20). However, the results in Fig. 2 B and in experiments in the following two sections are more compatible with a 10-d turnover rate for the donor-origin cDCs.

Antigenic phenotypes of donor-origin DCs in the blood and thymus

As in the parabiotic mice, almost all of the donor-origin cDCs in the thymus 2 d after i.v. transfer of blood cells were $Sirp\alpha^+$ $CD11b^+$ (Fig. 3). Of note, between 10 and 15% of the donor-origin pDCs and cDCs in the thymus at day 2 were MHC II^-, reflecting their frequency in the blood (unpublished data). This was also true at 6 h. As demonstrated in the section on monocytes (see below), the MHC II^- cDC precursors did not appear to be monocytes. Hence, although most of the pDCs and $Sirp\alpha^+$ $CD11b^+$ cDCs enter the thymus in a preformed state, committed DC precursors (21) also enter.

A more complete phenotypic analysis of the donor-origin DCs in the thymus at 48 h revealed that the pDCs were $CD11c^+$ $B220^+$ $PDCA^+$ $Gr\text{-}1^+$ MHC $II^{int/hi}$ $Sirp\alpha^{lo}$ $CD11b^-$ $CD8\alpha^{-/lo}$ $CD4^+$ $CD80^+$ $CD86^-$ $F4/80^-$ $NK1.1^-$, and the donor-origin cDCs were $CD11c^+$ $B220^-$ $PDCA^-$ $Gr\text{-}1^-$ MHC $II^{int/hi}$ $Sirp\alpha^{int/hi}$ $CD11b^+$ $CD8\alpha^-$ $CD4^+$ $CD80^{int/hi}$ $F4/80^-$ $NK1.1^-$. Of note, >50% of the donor-origin cDCs in the thymus were $CD86^+$, whereas their $Sirp\alpha^+$ $CD11b^+$ counterparts in the original inoculum were $CD86^-$. In addition, the proportion of donor-origin cDCs in the thymus that were MHC $II^{int/hi}$ increased progressively between 6 and 48 h, and greatly exceeded that in the original inoculum. These results suggest that thymus-homing cDCs, but not pDCs, mature shortly after entering the thymus. However, as shown in the following section, pDCs attain a semimature state and express CD8α between days 2 and 10.

Proliferation and maturation of thymus-homing DCs

In the course of these studies, we noted that two populations of DCs in the secondary lymphoid tissues of normal eGFP tg mice could be distinguished by their relative levels of GFP expression, the majority being GFP^{hi} and the minority being GFP^{lo} (Fig. 4 A). This was also true for the steady-state thymus, in which the GFP^{lo} and GFP^{hi} DCs exhibited relatively immature and mature antigenic phenotypes, respectively (unpublished data). Although GFP under the control of the actin promoter is not a specific marker for DC maturation, the GFP^{lo} thymic DCs appeared to be small round cells by light scatter analysis, and the GFP^{hi} DCs appeared to be either large round or large irregular cells. This was confirmed by the morphologies of FACS-sorted GFP^{lo} and GFP^{hi} thymic DCs, especially when subdivided into $CD11c^{lo}$ and $CD11c^{hi}$ subsets. Thus, as shown in Fig. 4 B, the GFP^{lo} $CD11c^{lo}$ DC fraction contained a mixture of small round and plasmacytoid cells, the GFP^{lo} $CD11c^{hi}$ fraction contained mostly medium-sized plasmacytoid cells, the GFP^{hi} $CD11c^{hi}$ fraction contained large DCs, and the GFP^{hi} $CD11c^{lo}$ fraction (not depicted) contained a mixture of large DCs and large plasmacytoid cells. Additionally, many of the DCs were undergoing mitosis, especially in the GFP^{hi} $CD11c^{hi}$ fraction. Strikingly, at day 2 after adoptive transfer, most of the donor-origin DCs in the thymus were GFP^{lo} (Fig. 4 C), whereas by day 10 ∼75% of the donor-origin DCs were GFP^{hi} (Fig. 4 D). It is unlikely that the GFP^{hi} DCs represented a separate migratory wave, as donor-origin GFP^{hi} DCs were rare in the blood at 48 h. Therefore, we presume that the GFP^{hi} donor-origin thymic pDCs and cDCs on day 10 were derived from the GFP^{lo} DCs.

Given the observed mitotic activity (Fig. 4 B), it was possible that proliferation played a role in the maturation process

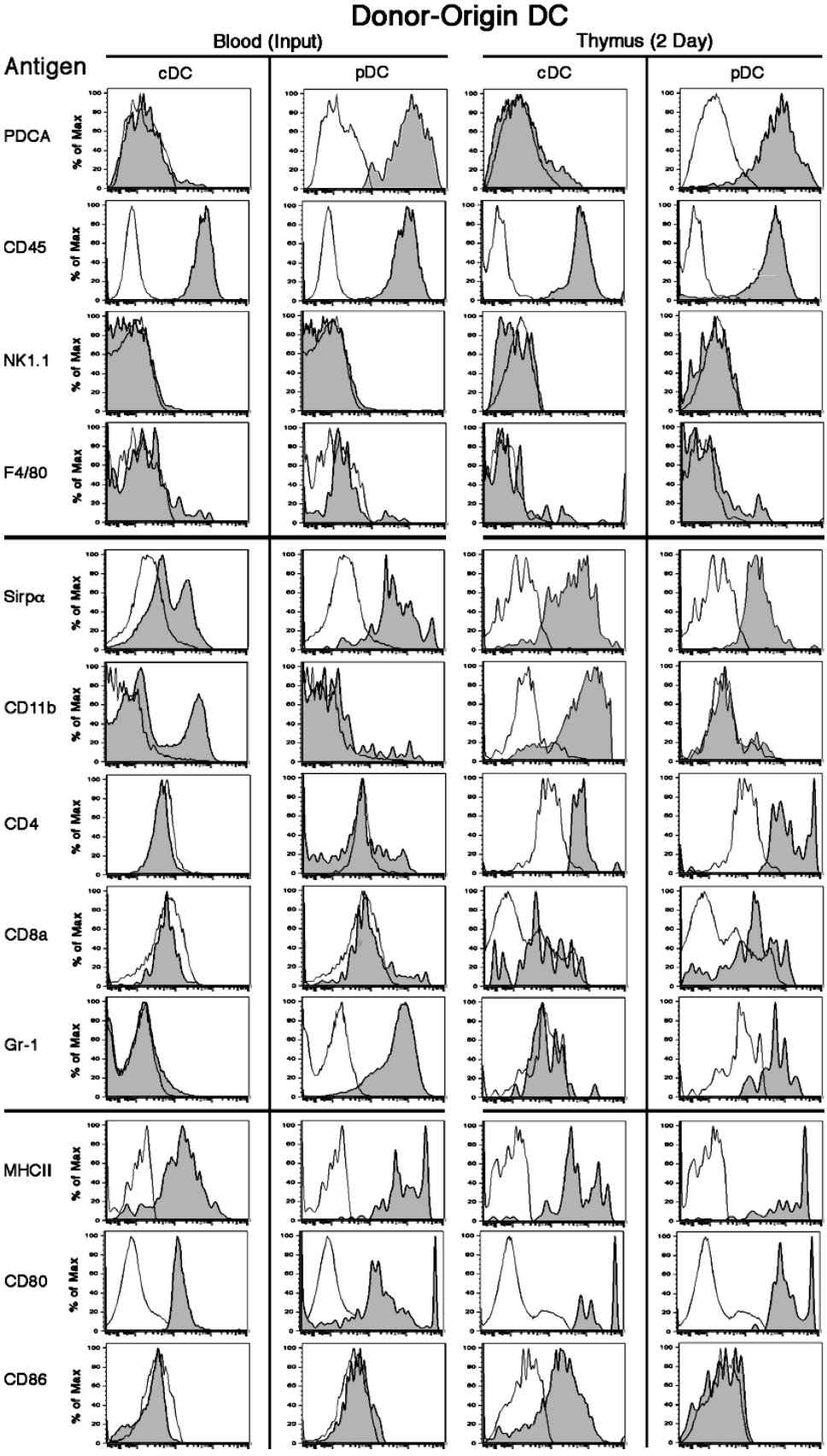
Donor-Origin DC
Blood (Input)
Thymus (2 Day)
Antigen
cDC
pDC
cDC
pDC
PDCA
CD45
NK1.1
F4/80
Sirpα
CD11b
CD4
CD8a
Gr-1
MHCII
CD80
CD86
% of Max

of the thymic-homing DCs. This appeared to be true for the cDCs, as <1% of the 7-aminoactinomycin D (7-AAD)–labeled $CD11b^+$ cDCs in the blood were cycling, whereas ~25% of the GFP^{lo} and 50% of the GFP^{hi} $CD11b^+$ cDCs in the steady-state thymus were in $S/G_2/M$ (Fig. 4 E). In contrast, the proportions of cycling pDCs in the blood and thymus were low (10–15%) and relatively constant. Thus, the $CD11b^+$ cDCs appeared to undergo a burst of proliferation shortly after entering the thymus but, as in the periphery (22), the pDCs did not. This was verified by adoptive transfer experiments (Fig. 4 F), in which ~45% of the donor-origin cDCs but only 15% of the donor-origin pDCs in the thymus were in cycle at 48 h. Overall, the immature thymus-homing $CD11b^+$ cDCs proliferated and differentiated into mature interdigitating DCs in the thymus, and the immature thymus-homing pDCs became semimature, possibly without the need for proliferation.

Monocytes fail to migrate to the thymus in the steady state

Monocytes have been shown to generate cDCs under inflammatory conditions (23–26), and it is possible that they may also do so in the steady state (27). Therefore, it was possible that some of the thymus-homing $CD11c^{lo}$ $CD11b^+$ $B220^-$ MHC II^- cells were monocytes rather than committed cDC precursors (21, 28, 29). This seemed unlikely, as <1% of these cells in normal blood labeled with anti–Gr-1 or anti-F4/80 (unpublished data), which reacts with both the $Gr\text{-}1^{hi}$ and $Gr\text{-}1^{lo}$ subsets of monocytes (30). Nonetheless, we could not exclude the possibility that a very small number of monocytes might have entered the thymus and generated $CD11b^+$ cDCs. We therefore directly determined whether immunomagnetically enriched eGFP tg monocytes (90–95% purity; Fig. 5 A), in numbers equal to those originally present among 20×10^6 bone marrow and blood cells, were able to migrate to the thymus after i.v. injection. As shown in Fig. 5 B, no donor-origin $CD11b^+$ (or $F4/80^+$) cells above background (≤0.1%) were seen in the thymus of monocyte recipients 2 d later. In contrast, donor-origin $CD11b^+$ cDCs (and pDCs) appeared in the recipients of unfractionated bone marrow (or blood) and the monocyte-depleted cell fraction. To further exclude a role for monocytes in the generation of thymic $CD11b^+$ cDCs, we examined the donor-origin cells present 2 and 10 d after the injection of purified monocytes i.v. or directly into the thymus (intrathymically). No donor-origin cDCs, pDCs, or monocytes were found 2 or 10 d after either intrathymic injection (Fig. 5 C) or i.v. injection (not depicted). In contrast, all of these cell populations were present 10 d after the intrathymic injection of unfractionated or monocyte-depleted bone marrow cells.

Noninflammatory DCs can transport circulating antigens from the blood to thymus

We and others have shown that inflammatory DCs can transport antigens from the periphery to the thymus (see Discussion). In this study, we demonstrate that this can also occur with noninflammatory DCs. In these experiments, CD45.2 mice were injected i.v. with 0.5 mg of soluble Alexa Fluor 488–OVA, and the blood and thymus were harvested 18 h later. As shown in Fig. 6 A, ~15% of the pDCs and 35% of the $CD11b^+$cDCs in the blood were OVA^+. These cells did not appear to be activated, as judged by their failure to up-regulate CD80, CD86, or MHC II (unpublished data). However, because of the diffusion of OVA into the thymus, as indicated by labeling of the $CD11b^-$ cDCs (Fig. 6 A), it was not possible to determine whether any thymus-homing DCs had transported OVA from the blood to thymus. We therefore transferred 20×10^6 of the blood cells from the OVA-injected mice into CD45.1 recipients. After 24 h, ~4% of the pDCs and 1% of the $CD11b^+$ cDCs but none of the $CD11b^-$ cDCs in the thymus were OVA^+ (Fig. 6 B). Comparable results were obtained when spleen cells labeled in vivo with circulating OVA were adoptively transferred. In both instances, only donor-origin thymic DCs were OVA^+.

In a set of parallel experiments, 2-μm fluorescent microspheres were injected i.v., and their transport by DCs to the thymus was examined 18 h later. The results in Fig. 6 C show that, unlike soluble OVA, there was little direct uptake of the microspheres by the resident $CD11b^-$ cDC subset in the thymus. Yet, ~2.5% of the pDCs and 2% of the $CD11b^+$ cDCs contained microspheres, presumably acquired in the periphery.

Developmental dissociation of thymic DCs of intrathymic and extrathymic origin

The present results indicate that the populations of pDCs and $Sirp\alpha^+$ $CD11b^+$ cDCs in the normal thymus arise independently of the population of $Sirp\alpha^-$ $CD11b^-$ cDCs, and that the latter arises intrathymically from a common T cell/DC progenitor. Two experimental approaches are taken in this study to verify this formally. The first approach takes advantage of our observation that the migration of thymocyte progenitors to the thymus is a gated process having a periodicity of ~4 wk (18). The second approach is based on our observation that similar numbers of $CD8\alpha^{-/lo}$ $IL\text{-}7R\alpha^{-/-}$ DCs and $CD8\alpha^{hi}$ WT DCs appear in the thymus of nonirradiated $IL\text{-}7R\alpha^{-/-}$ mice injected i.v. with WT bone marrow cells (unpublished data) (31). In the first approach, groups of nonirradiated WT mice ranging from 5 to 9 wk of age were injected i.v. with 20×10^6 $eGFP^+$ tg WT bone marrow cells, and the levels of donor-origin DCs and thymocyte chimerism

Figure 3. Surface phenotypes of donor-origin DCs in the blood and thymus of adoptive recipients. 20 million blood cells from $eGFP^+$ tg mice (input) were injected i.v. into normal WT recipients. After 2 d, blood and thymus cells were harvested and stained for CD11c, B220, Sirpα, and one of the other listed surface antigens. The markers were divided into three groups: (top) PDCA, CD45, NK1.1, and F4/80 to confirm that the $CD11c^+$ cells were cDCs and pDCs; (middle) Sirpα, CD11b, CD4, CD8α, and Gr-1 for DC subset identification; and (bottom) MHC II, CD80, and CD86 expression levels for maturity and activation. Background fluorescence with only the relevant antibody omitted is shown by the unshaded profile. Representative analyses from two to eight experiments are shown.

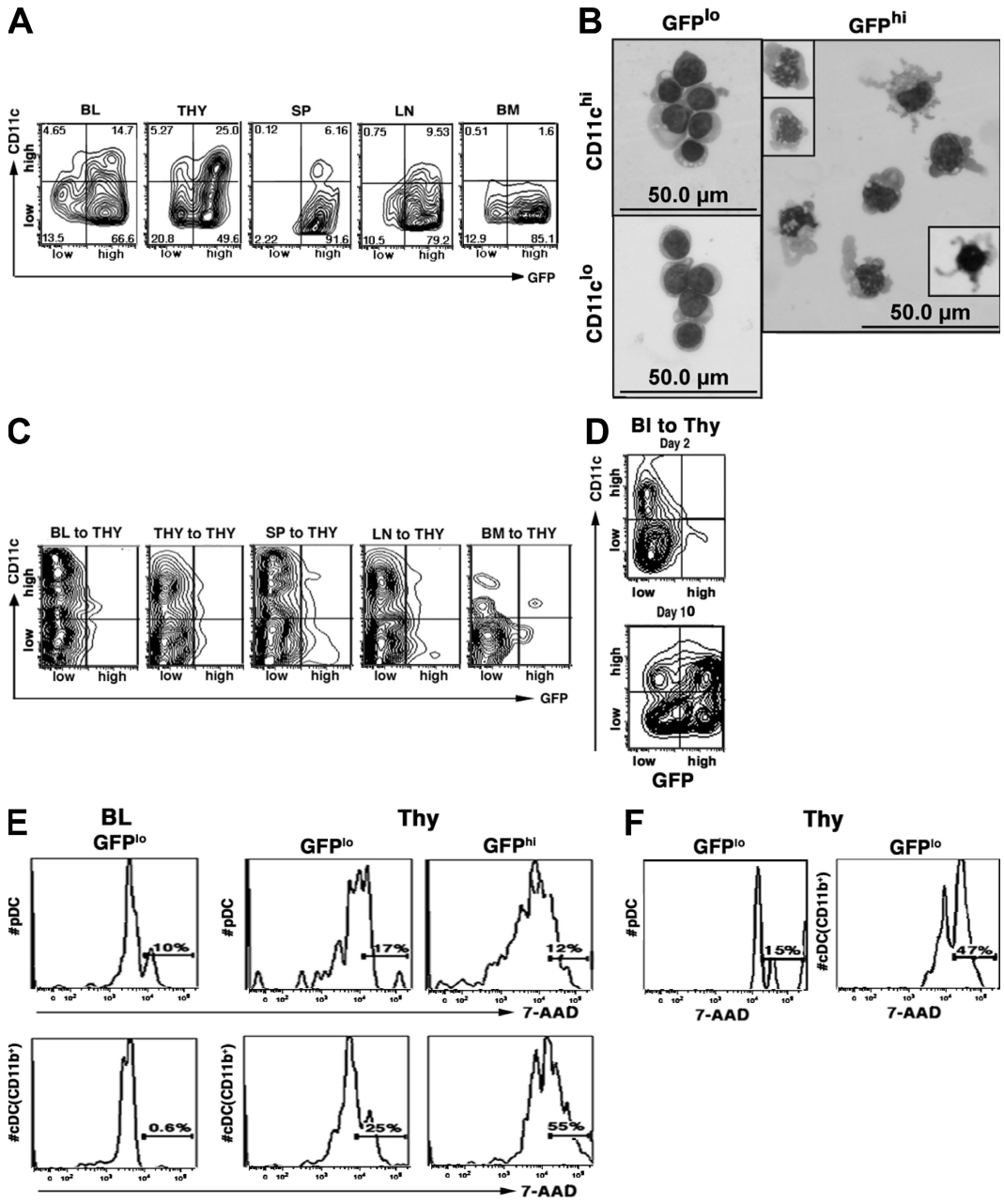

Figure 4. Activation, maturation, and proliferation of the DCs that enter the thymus. (A) Distribution of DCs in the blood, thymus, spleen, lymph nodes, and bone marrow from normal eGFP tg mice according to relative fluorescence intensity (high/low) for GFP and CD11c. The numbers indicate the percentage of total DCs present in each quadrant of the fluorescence profile. Only the $CD11c^+$ GFP^+ cells are shown. Representative profiles from five mice are shown. (B) Giemsa-stained cytocentrifuged suspensions of thymic DCs from normal eGFP tg mice sorted by FACS according to relative fluorescence intensity (high/low) for GFP and CD11c. Insets in the panel of GFP^{hi} $CD11c^{hi}$ DCs show mitotic figures (left) and a well-differentiated DC with prominent dendritic processes (right). A representative experiment (one out of three) is shown. (C) Distribution of the donor-origin DCs present in the thymus 2 d after i.v. injection of 20×10^6 eGFP tg blood, spleen, lymph node, bone marrow, or thymus cells into normal WT recipients according to relative fluorescence intensity (high/low) for GFP and CD11c. Only the $CD11c^+$ GFP^+ cells are shown. Representative profiles from one out of three experiments are shown. (D) Distribution of the donor-origin DCs present in the thymus 2 and 10 d after i.v. injection of 20×10^6 $eGFP^+$ blood cells according to relative fluorescence intensity (high/low) for GFP and CD11c (note similarities between the profiles of donor-origin DCs at day 10 with that of total DCs in the normal thymus, as shown in A). Representative profiles from one out of two experiments (five mice each) are shown. (E) Cell-cycle analysis with 7-AAD of the GFP^{lo} (immature) and/or GFP^{hi} (mature) subsets of pDCs and $CD11b^+$ cDCs in the blood and thymus of normal eGFP tg mice. The percentages of cells in $S/G_2/M$ are indicated. Representative profiles from one out of two experiments (three mice each) are shown. (F) Cell-cycle analysis of the donor-origin DCs present in the thymus 2 d after adoptive transfer of 20×10^6 eGFP tg blood cells into normal WT recipients. 7-AAD staining of donor-origin pDCs and $CD11b^+$ cDCs. The percentages of cells in $S/G_2/M$ are indicated. Representative profiles from one out of two experiments (three mice each) are shown.

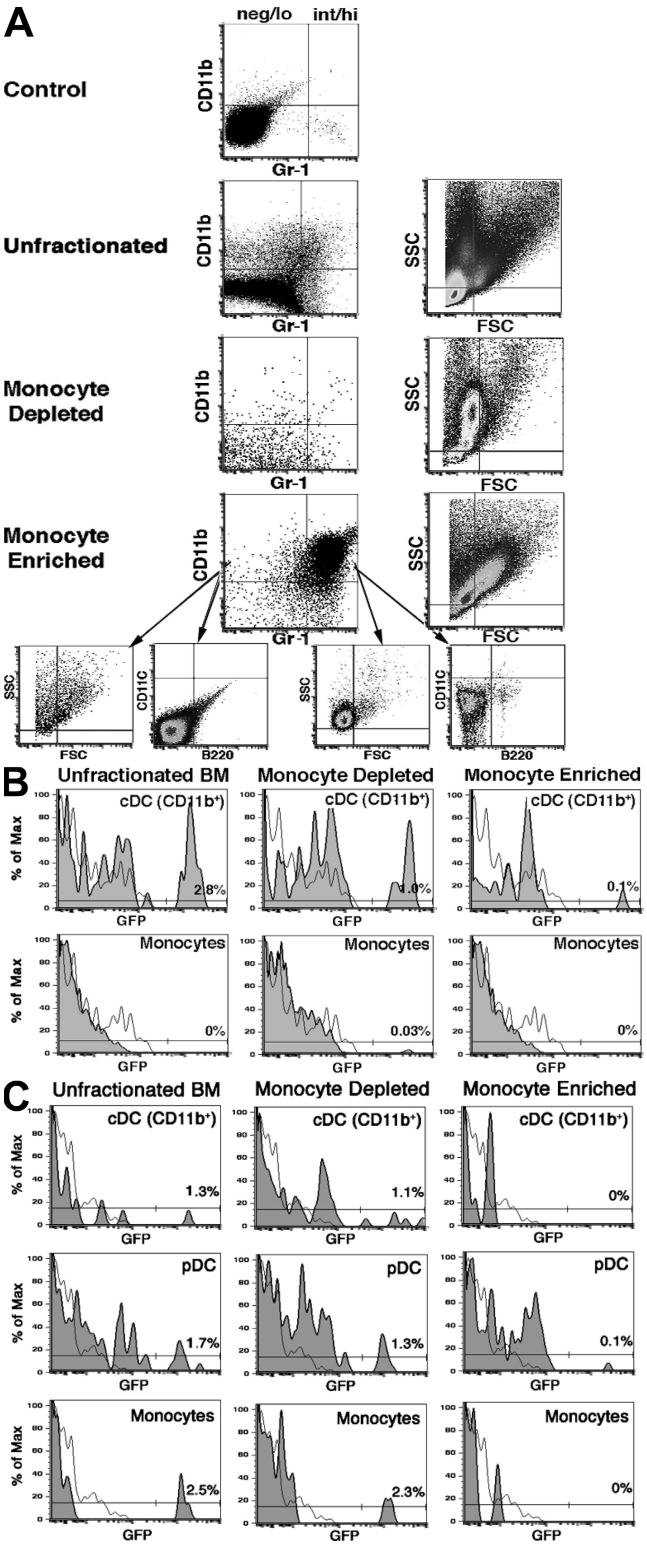

Figure 5. Monocytes do not migrate to the steady-state thymus. (A) Enrichment of monocytes from the blood. Unfractionated blood cells were sorted into monocyte-enriched (90–95% purity) and monocyte-depleted populations by immunomagnetic separation for MHC II, B220, CD43, and CD24 (see Materials and methods). Approximately 90% of the monocytes were Gr-1$^{int/hi}$ and 10% were Gr-1$^{neg/lo}$. Each fraction was further characterized by light scatter analysis and CD11c expression. A representative experiment (one out of four) is shown. (B) Monocytes do not migrate to the thymus. 20 million unfractionated eGFP tg blood cells, 2×10^6 monocyte-enriched blood cells, or 18×10^6 monocyte-depleted blood cells were injected i.v. into normal WT recipients. The proportions of the total CD11b$^+$ thymic cells at 2 d that were donor-origin cDCs (CD11c$^+$Gr-1$^-$F4/80$^-$) and/or monocytes (CD11c$^-$Gr-1^{-or+}F4/80$^+$) were determined for each inoculum (percentages are indicated). A representative experiment (one out of three) is shown. (C) Monocytes do not generate DCs when injected directly into the thymus. Two million unfractionated, 0.2×10^6 monocyte-enriched, or 1.8×10^6 monocyte-depleted eGFP tg blood cells were injected into the thymus of normal WT recipients. After 10 d, the proportions of the total pDCs, CD11b$^+$ cDCs, or monocytes that were of donor origin were determined (percentages are indicated). A representative experiment (one out of two) is shown.

were determined 2 and 30 d later. The results in Table I show that donor-origin pDCs and Sirpα^+ CD11b$^+$ cDCs entered the thymus of mice of all ages by day 2, but only the groups of mice that developed thymocyte chimerism (the 8- and 9-wk-old recipients) contained donor-origin cDCs on day 30. However, unlike the Sirpα^+ CD11b$^+$ CD8α^- cDCs seen on day 2, most of the donor-origin cDCs present on day 30 had a Sirpα^- CD11b$^-$ CD8α^{hi} phenotype.

In the second approach, nonirradiated IL-7R$\alpha^{-/-}$ mice (CD45.2) were injected i.v. with 20×10^6 CD45.1 WT bone marrow cells, and the thymus cells were harvested 6 wk later. As shown in Table II, large numbers of WT thymocytes and WT DCs were present, the latter being mostly Sirpα^- CD11b$^-$ CD8α^{hi} cDCs. In contrast, few IL-7R$\alpha^{-/-}$ thymocytes but large numbers of IL-7R$\alpha^{-/-}$ pDCs and cDCs were present, the latter being mostly Sirpα^+ CD11b$^+$ CD8α^-. Consequently, the WT and IL-7R$\alpha^{-/-}$ populations of thymic DCs appeared to have different developmental origins, with only the former being associated with thymocyte formation.

In a variation of this model, sublethally irradiated (6 Gy) CD45.1 WT recipients were injected i.v. with 20×10^6 CD45.2 Rag$^{-/-}$ bone marrow cells alone or mixed with an equal number of CD45.2 eGFP tg WT bone marrow cells. Although few Rag$^{-/-}$ thymocytes were generated, expanded numbers of Rag$^{-/-}$ DCs appeared in the host thymus, as previously reported (32). Again, most of the WT DCs were Sirpα^- CD11b$^-$ CD8α^{hi} cDCs and most of the Rag$^{-/-}$ DCs were pDCs and Sirpα^+ CD11b$^+$ CD8α^- cDCs (Table III).

DISCUSSION

Wu and Shortman (1) have described three phenotypically distinct populations of DCs in the normal mouse thymus: (a) pDCs, (b) SIRPα^+ CD11b$^+$ CD8$\alpha^{-/lo}$ cDCs, and (c) SIRPα^- CD11b$^-$ CD8α^{hi} cDCs. The present study indicates that two of these thymic DC subsets, namely pDCs and Sirpα^+ CD11b$^+$ cDCs, arise extrathymically and continually migrate from the blood to thymus. Vandenabeele et al. (33) have proposed a similar scenario regarding the CD11b$^+$ subset of cDCs in the human thymus. Strictly speaking, many of the mature Sirpα^+

$CD11b^+$ cDCs in the thymus probably are formed intrathymically by proliferating $Sirp\alpha^+$ $CD11b^+$ MHC II^{lo} cDCs and/or their $Sirp\alpha^+$ $CD11b^+$ MHC II^- precursors that have emigrated from the blood. However, for convenience we refer to this cDC subset as being of extrathymic origin.

In contrast, the $Sirp\alpha^-$ $CDllb^-$ $CD8\alpha^{hi}$ subset of thymic cDCs appears to arise entirely within the thymus, presumably from a common T cell/DC precursor. This was shown by age–response experiments in which the $Sirp\alpha^-$ $CD11b^-$ $CD8\alpha^{hi}$ subset of donor-origin cDCs appeared in the thymus only when the "gates" for thymocyte progenitor entry were open (18), and by developmental studies in which the vast majority of WT DCs that formed after transfer of WT bone marrow cells into nonirradiated IL-$7R\alpha^{-/-}$ mice or of $Rag^{-/-}$ bone marrow cells into irradiated WT recipients were $Sirp\alpha^-$ $CD11b^-$ $CD8\alpha^{hi}$. These results are consistent with earlier precursor-product studies of "low CD4" thymocyte precursors and $CD8^{-/lo}$ and $CD8^{hi}$ thymic cDCs (1, 34), as well as with adoptive transfer experiments involving $Rag^{-/-}$, Notch-$1^{-/-}$, Tef-$1^{-/-}$, and IL-$7R\alpha^{-/-}$ mice (32, 34–36). They are also consistent with the observation that the earliest intrathymic thymocyte progenitors ($CD4^{lo}$) did not generate significant numbers of thymic pDCs upon in vivo transfer, although they could readily generate cDCs (unpublished data). However, they differ from the observation of Weijer et al. (37) that $CD34^+$ cells generated pDCs when injected i.v. or directly into human fetal thymus fragments in $RAG^{-/-}$ $\gamma c^{-/-}$ mice. It is possible, of course, that the latter results may not be applicable to the intact adult mouse thymus and, in the case of i.v. injection, may be explained by the migration of extrathymically generated pDCs to the thymus. Similarly, Ito et al. (38) have reported that IL-18 or a combination of IL-1β, IL-3, and TNF-α induced the in vitro generation of $CD11b^+$ $CD8\alpha^-$ cDCs from fetal or adult DN1 and DN2 thymocytes, respectively (39). However, their experiments did not address the question of the origins of $CD11b^+$ thymic cDCs in vivo.

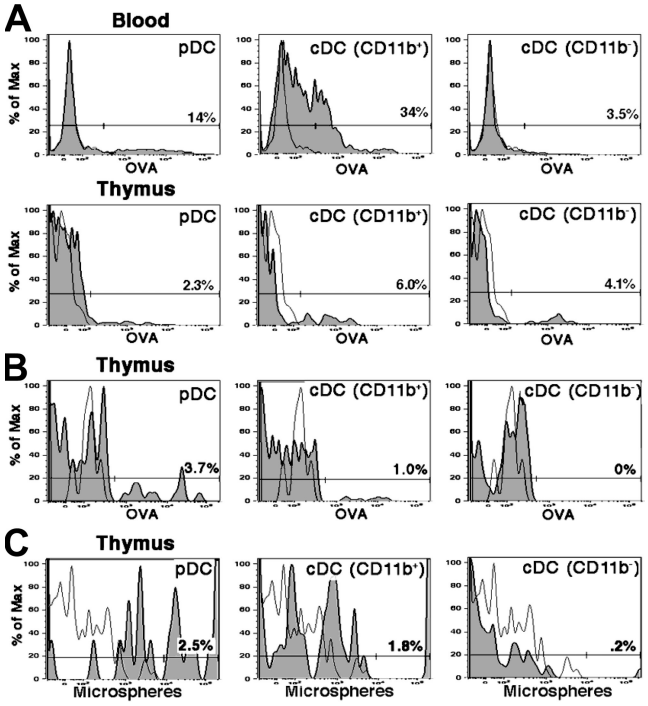

Figure 6. DCs transport circulating OVA and microspheres to the thymus. (A) In vivo uptake of circulating soluble OVA by DCs in the blood and thymus. Normal WT mice were injected i.v. with 0.5 mg Alexa Fluor 488–OVA, and the percentages of total pDCs, $CD11b^+$ cDCs, and $CD11b^-$ cDCs in the blood and thymus that were OVA^+ were determined by FACS analysis 18 h later. A representative experiment (one out of three) is shown. (B) Migration of OVA^+ DCs to the thymus of adoptive recipients. 20 million nucleated blood cells from WT CD45.2 mice that had been injected i.v. with 0.5 mg OVA 18 h previously (as in A) were washed and transferred i.v. into normal WT CD45.1 recipients. After 24 h, the percentages of the total pDCs, $CD11b^+$ cDCs, and $CD11b^-$ cDCs in the thymus that were OVA^+ were determined. All of the OVA^+ DCs were of donor origin. Representative profiles from one out of two experiments are shown. (C) Experiments were performed as in A, except that 2-μm Fluoresbrite microspheres were substituted for soluble OVA. A representative experiment (one out of two) is shown.

In dose–response experiments, the migration of both pDCs and $Sirp\alpha^+$ $CD11b^+$ cDCs to the thymus obeyed strict saturation kinetics, suggesting that the adult thymus has a finite number of niches for immigrating DCs. In addition, the seeding efficiencies to the thymus of pDCs and $Sirp\alpha^+$ $CD11b^+$ cDCs from the blood, spleen, lymph nodes, and bone marrow approximated 10% when the proportions of the input numbers of DCs that entered the thymus within 2 d were calculated. However, in the case of GFP^{lo} (immature) thymic DCs (the GFP^{hi} [mature] DCs did not return to thymus), the seeding efficiency approximated 50%. This striking result is consistent with that of Duncan et al. (19) but differs from that of Bonasio et al. (40), who reported that splenic DCs were recruited to the thymus with efficiencies equal to or better than that of thymic DCs and that all subsets of splenic DCs had thymus migratory activity. Although the reasons for these differences are unclear, it should be noted that Flt-3L–stimulated DCs were used in the latter experiments and that the numbers of DCs transferred ($5–20 \times 10^6$) greatly exceeded those routinely used in this study ($\sim 5 \times 10^5$). However, we cannot exclude the possibility that a very small proportion of the cDCs that reached the thymus in our experiments had a $Sirp\alpha^-$ $CD11b^-$ $CD8\alpha^{hi}$ phenotype.

In agreement with the present results, Liu et al. (41) have recently reported that most DCs are not exchanged randomly between parabiotic partners, presumably because they have a short half-life in the blood. In the present study, we identified the DCs that were randomly exchanged between parabiotic partners as immature pDCs and $Sirp\alpha^+$ $CD11b^+$ $CD8\alpha^{-/lo}$ cDCs. In addition, Liu et al. found that the DCs in the blood were in equilibrium with those in the spleen and lymph nodes, suggesting that most DCs in these organs were derived from circulating precursors. We previously observed a similar phenomenon regarding the equilibration of thymocyte progenitor activity between the blood and thymus of parabiotic mice (15). In this study, we demonstrate that the circulating pDCs and $Sirp\alpha^+$ $CD11b^+$ cDCs reached equilibrium with their counterparts in the thymus within 3 wk after parabiotic union.

The reasons for the selective migration of pDCs and $SIRP\alpha^+$ $CD11b^+$cDCs to the steady-state thymus are not

Table I. DC chimerism in the thymus as a function of age

	Donor-origin cells (days after transfer)							
	Day 2				Day 30			
Age of recipients	Thymocytes[a]	% of cDCs[b]	% of pDCs	% of total DCs	Thymocytes[a]	% of cDCs[c]	% of pDCs	% of total DCs
5 wk	–	14.6 ± 3.6	84.4 ± 8	7.1 ± 0.4	–	<1	98.3 ± 13.1	0.5 ± 0.1
6 wk	–	16.1 ± 13.2	82.9 ± 27.2	5 ± 1.3	–	<1	99.1 ± 3.9	0.1 ± 0
7 wk	–	18.6 ± 5.4	80.4 ± 3.7	5.3 ± 2.4	–	<1	95.1 ± 3.3	0.1 ± 0.01
8 wk	–	18.3 ± 2	80.7 ± 14.8	8.4 ± 0.3	+	84.5 ± 9.3	15.5 ± 9.3	11.9 ± 2.4
9 wk	–	16.5 ± 5.9	82.4 ± 9.5	5.1 ± 0.6	+	52.8 ± 3.9	47.2 ± 3.9	4.5 ± 0.1

[a]–, <1% $CD3^+$ donor-origin thymocytes; +, >5% $CD3^+$ donor-origin thymocytes.
[b]>95% $Sirp\alpha^+$ $CD11b^+$ $CD8\alpha^{-/lo}$ cDCs.
[c]>95% $Sirp\alpha^-$ $CD11b^-$ $CD8\alpha^{hi}$ cDCs.

known but presumably are related to the expression of a novel combination of adhesion molecules and chemotactic receptors (40). It is also possible that Sirpα itself is involved in this migratory behavior, as Sirpα signaling modulates transendothelial and transepithelial migration and enables $Sirp\alpha^+$ DCs (both pDCs and cDCs) to traverse the high endothelial venules in the lymph nodes (42, 43). Significantly, the increased migration of immature DCs through high endothelial venules has been reported to enhance the induction of antigen-specific T reg cells in lymph nodes (44, 45), possibly because the Sirpα protein, when engaged by its ligand (CD47), causes a shift in cytokine profiles and the formation of semimature DCs (22, 46). A similar function in the thymus could theoretically lead to the development of antigen-specific T reg cells (38).

Unlike the situation in the peripheral lymphoid tissues, the $Sirp\alpha^+$ $CD11b^+$ cDCs that enter the thymus up-regulate CD80 and CD86 as well as CD11c and MHC II. In addition, they proliferate extensively and differentiate into mature interdigitating cDCs over a 10-d period. Intriguingly, Watanabe et al. (47) have reported that thymic stromal lymphopoietin–producing medullary epithelial cells stimulated some thymic DCs to up-regulate MHC II, CD80, and CD86, and induce the formation of $CD4^+$ $CD25^+$ $Foxp3^+$ thymic T reg cells. The present experiments raise the possibility that the subset of $Sirp\alpha^+$ $CD11b^+$ cDCs may participate in this phenomenon, as it was the only DC subset that underwent large-scale activation in the steady-state thymus. Indeed, Proietto et al. (11) have recently reported that $Sirp\alpha^+$ $CD11b^+$ cDCs from the thymus but not the spleen induced $CD4^+$ $CD25^+$ $Foxp3^+$ T reg cells from $CD4^+$ $CD25^-$ $Foxp3^-$ thymocytes but not splenocytes in vitro, suggesting that this phenomenon was thymus specific. They also demonstrated that, unlike splenic cDCs, both the $Sirp\alpha^+$ and $Sirp\alpha^-$ subsets of thymic cDCs could acquire and cross-present cell-associated OVA to CD8 OT-1 T cells, and that both thymic DC subsets were superior to their splenic counterparts in presenting OVA on MHC II to CD4 OT-II T cells (48). Furthermore, given that pDCs achieve a semimature status after migration to the thymus, the possibility also exists that they too may be able to induce T reg cells and/or NKT reg cells in the thymus, much as they do in the periphery (12–14, 38, 49–51).

In this respect, many investigators have shown that inflammatory DCs can migrate to the thymus and induce $CD4^+$ $CD25^+$ T reg cells and/or activate NKT reg cells. For example, Khoury et al. (52) demonstrated that thymic DCs pulsed in situ with myelin basic protein induced protective antigen-specific $CD4^+$ $CD25^+$ T reg cells when infused into naive

Table II. Subsets of IL-7R$\alpha^{-/-}$ and WT DCs in the thymus of adoptive recipients[a]

IL-7R$\alpha^{-/-}$ recipients of WT bone marrow cells			pDCs	cDCs	
Origin of cells	Number of thymocytes	Number of DCs	$Sirp\alpha^+$ $CD11b^-$ $B220^+$	$Sirp\alpha^+$ $CD11b^+$ $CD8\alpha^{-/lo}$	$Sirp\alpha^-$ $CD11b^-$ $CD8\alpha^{hi}$
	$x10^{-6}$	$x10^{-3}$	%	%	%
WT	54.3 ± 8.9[b]	27 ± 11.1[c]	5.7 ± 1.8[b,c]	6.7 ± 2.8[b,c]	87.5 ± 7[b,c]
IL-7R$\alpha^{-/-}$	0.8 ± 0.3	33.4 ± 3.5[d]	29.8 ± 0.7[d]	67 ± 3.6[d]	4.2 ± 1.2[d]
WT control	93.2 ± 13	60.5 ± 12.1	38.7 ± 3.7	22.2 ± 7.5	39.1 ± 7.3

[a]Data were analyzed 6 wk after adoptive transfer of WT bone marrow cells into nonirradiated IL-7R$\alpha^{-/-}$ recipients.
[b]$P < 0.01$ between WT and IL-7R$\alpha^{-/-}$.
[c]$P < 0.01$ between WT and WT control cells.
[d]$P < 0.01$ between IL-7R$\alpha^{-/-}$ and WT control cells.

Table III. Subsets of $Rag^{-/-}$ and WT DCs in the thymus of adoptive recipients[a]

WT recipients of $Rag^{-/-}$ and/or WT bone marrow			pDCs	cDCs	
Origin of cells	Number of thymocytes	Number of DCs	$Sirp\alpha^+$ $CD11b^-$ $B220^+$	$Sirp\alpha^+$ $CD11b^+$ $CD8\alpha^{-/lo}$	$Sirp\alpha^-$ $CD11b^-$ $CD8\alpha^{hi}$
	$x10^{-6}$	$x10^{-3}$	%	%	%
WT	134.5 ± 23.1[b]	99.7 ± 17.6[b]	21.6 ± 6.2[b]	14.8 ± 3.2	63.7 ± 4.3[b,c]
$Rag^{-/-}$	2.2 ± 0.5[d]	15.3 ± 4.8[d]	66.3 ± 0.8[d]	22 ± 1.6	11.6 ± 1[d]
WT plus $Rag^{-/-}$	116.2 ± 24[b] plus 1.6 ± 0.2	69.6 ± 10.9[b] plus 28.5 ± 3.2	13.1 ± 0.8[b,c] 60.0 ± 6.1[d]	13 ± 1.2[b,c] 28.4 ± 4.7	71.9 ± 4.9[b,c] 11.5 ± 1.6[d]
WT control	149.2 ± 28.1	97.8 ± 16.4	36.5 ± 0.6	24.1 ± 3.4	38 ± 5.2

[a]Data were analyzed 4 wk after adoptive transfer of $Rag^{-/-}$ and/or WT bone marrow cells into 6-Gy–irradiated WT recipients.
[b]$P < 0.01$ between WT and $Rag^{-/-}$ cells.
[c]$P < 0.01$ between WT and WT control cells.
[d]$P < 0.01$ between $Rag^{-/-}$ and WT control cells.

euthymic, but not thymectomized, mice. Other investigators have reported that the migration of donor-origin DCs to the thymus after heart, lung, and renal allografting was associated with the formation of MHC II–allospecific $CD4^+$ $CD25^+$ T reg cells (19, 53). A similar mechanism may play a role in establishing tolerance by pretransplant infusion of donor lymphoid cells (54–56). Indeed, migration of semiallogeneic DCs to the thymus after treatment with CSA or LF15-0195 has been found to expand $CD4^+$ $CD25^+$ $Foxp3^+$ T reg cells (8, 57); we have also observed the formation of self–MHC II–specific $CD4^+$ $CD25^+$ thymic T reg cells that prevent autologous graft-versus-host disease in CSA-treated mice (6, 7). We have also observed that circulating $F4/80^+$ antigen-presenting cells activate NKT reg cells in the thymus after the intraocular injection of foreign antigen (unpublished data) (4, 5). Some of these and related observations have already been applied therapeutically in the management of autoimmune disorders and the prevention of allograft rejection (19, 58, 59).

This then leaves the question of the functions of thymus-homing DCs in the steady state. We have previously postulated that noninflammatory DCs, like inflammatory DCs, are involved in inducing dominant and deletional thymic tolerance by transporting and presenting peripheral self- and non-self-antigens to the thymus (2, 10). The present study identifies a mechanism by which this might occur by demonstrating (a) the existence of a physiological blood-to-thymus migration pathway for noninflammatory pDCs and $Sirp\alpha^+$ $CD11b^+$ cDCs, (b) the ability of these DCs to acquire and transport circulating antigen to the thymus, and (c) the ability of these DCs to differentiate into semimature pDCs and mature cDCs once in the thymus. That these thymic-homing DCs constitute fully one half of the DCs normally found in the adult thymus further attests to their probable importance in thymic function. Furthermore, as circulating immature DCs routinely capture bloodborne antigens, and some tissue-resident DCs enter the blood after acquiring antigen (60), it seems likely that DCs routinely transport antigen to the thymus, much as they do to the secondary lymphoid tissues. Support for this notion has recently been provided by Bonasio et al. (40, 61), who detected antigen-specific deletional tolerance in the thymus of recipients of immature OVA-pulsed DCs. These investigators also observed central deletional tolerance to membrane-bound OVA on cardiac myocytes in OT-II bone marrow radiation chimeras, presumably because of thymus-homing DCs. Additionally, Proietto et al. (11) have recently attributed the occurrence of both negative selection and the induction of antigen-specific T reg cells in the thymus of $Rag2^{-/-}$OTII/CD11c OVA double-tg bone marrow chimeras to the migration of peripheral DCs to the thymus.

An especially rich source of tissue-specific self-antigens for thymus-homing DCs could be apoptotic cells, which express CD47, the ligand for Sirpα (46, 60, 62). In addition, the establishment by thymus-homing DCs of central tolerance to innocuous foreign antigens might be of special importance, as most of these antigens would not be ectopically expressed in and might not otherwise reach the thymus. Nonetheless, given the apparently broad diversity of the TCR repertoires of intrathymically generated T reg cells (63), T reg cells that down-regulate immune responses to toxic or pathogenic antigens might also be formed. Under these circumstances, the induction of peripheral immunity and dominant central tolerance would have to be tightly coordinated so as to permit effective protection while preventing excessive tissue damage (64, 65). We have previously observed such a phenomenon in the formation and release of waves of purified protein derivative– and OVA-specific "suppressor" T cells from the thymus on days 4 and 9–12, respectively, after the induction of an immune response to the footpad injection of OVA in CFA (unpublished data) (66). Hence, it can be envisioned that dominant and/or deletional thymic tolerance to a broad spectrum of extrathymically expressed antigens is induced continuously by thymus-homing DCs in the steady state (Fig. 7), as well as being induced intermittently in the inflammatory state. In the latter instance, it is possible that monocyte-derived DCs may be involved (unpublished data). However, until definitive functional studies are conducted, the precise roles of the thymus-homing DCs in the steady state remain speculative.

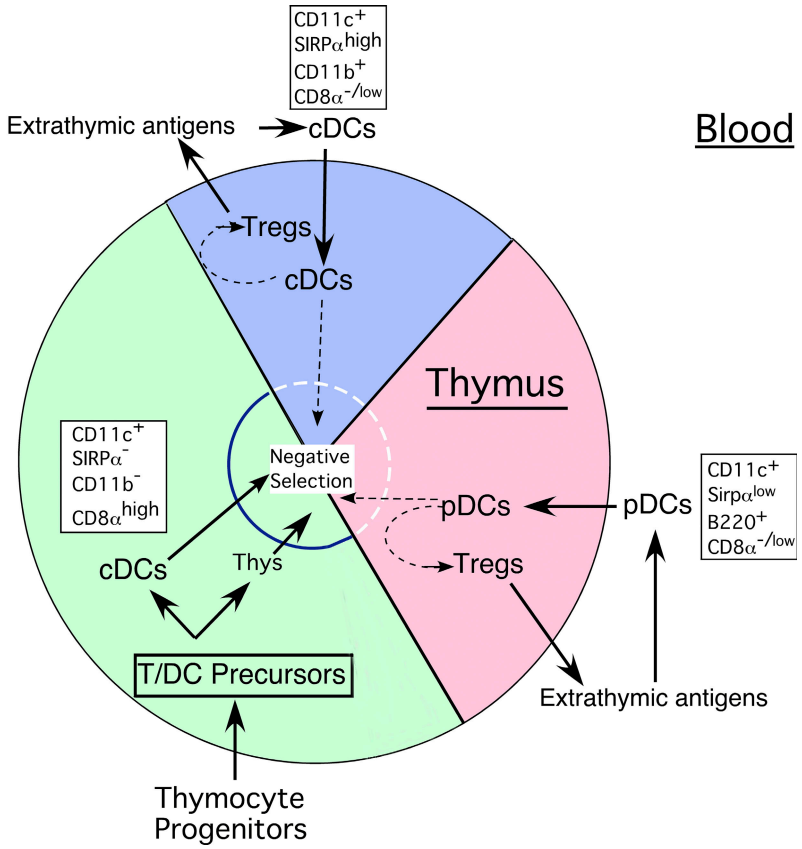

Figure 7. Functional implications of the blood–to–thymus migration pathway for DCs in the steady state. In this scheme, ∼50% of the total DCs in the steady-state thymus represent and/or arise from thymus-homing immature DCs or their immediate MHC II$^-$ precursors in the blood. Virtually all of the pDCs and approximately one third of the cDCs in the thymus originate in this manner. The thymus-homing cDCs can be distinguished from the major population of intrathymic cDCs by the expression of Sirpα and CD11b, and the lack of expression of CD8α. Immature thymus-homing pDCs and cDCs acquire and process self- and nonself-antigens in the periphery under noninflammatory conditions and transport them to the thymus. Once in the thymus, (a) the pDCs and Sirpα$^+$ CD11b$^+$ cDCs occupy recently vacated niches in the medullary and corticomedullary regions, (b) the pDCs develop a semimature phenotype, and (c) the cDCs undergo activation, proliferation, and maturation into fully differentiated DCs. We propose as a working hypothesis that one or both of these thymus-homing DC populations assist, directly or indirectly, in the induction of antigen-specific CD4$^+$ CD25$^+$ Foxp3$^+$ T reg cells and/or in antigen-specific negative selection. As a consequence, the diversity of the TCR repertoire of T reg and effector T cells in the thymus is continually altered to reflect the changing antigenic milieu in the periphery, especially to myriad foreign and some tissue-specific antigens that are not ectopically expressed by the thymic epithelium.

MATERIALS AND METHODS

Animals. Congenic Ly5.1 C57BL/6N and B6-Ly5.2/Cr mice were purchased from Charles River Laboratories. Breeding pairs of B6 eGFP tg mice (actin promoter) were provided by T. Randall (Trudeau Institute, Inc., Saranac Lake, NY). Rag$^{-/-}$ (B6.129S7-RagltmlMom/J) and breeding pairs of 1L7Rα$^{-/-}$ (B6.129S7-1L7rtm11mx/J) mice were purchased from the Jackson Laboratory. Animals were used between 5 and 8 wk of age unless otherwise indicated. All animals were maintained by the Center for Laboratory Animal Care of the University of Connecticut Health Center and were used according to protocols approved by the Institutional Animal Care and Use Committee.

Antibodies and flow immunocytometry. FITC-, PE-, PerCpCy5.5-, allophycocyanin (APC)-, APC-Cy7–, Pacific blue–, and biotin-conjugated rat monoclonal antibodies against mouse Gr-l, CD11c, CD11b (MAC-1), B220 (CD45R), F4/80, TCR, CD3, CD4, CD43, CD45.1 (Ly5.2), and CD45.2 (Ly5.1) were purchased from BD. Conjugated antibodies to CD8α, CD80, CD86, MHC II, PDCA, and CD24 were purchased from eBioscience. Biotinylated anti-SIRPα was a gift from W. Li (Walter and Eliza Hall Institute, Melbourne, Australia). The expression of these antigens (and GFP) was determined by simultaneous three- to five-color fluorescence analysis on a flow cytometer (FACSCalibur, modified FACScan, or LSR II; BD). Three-color analyses were done using FITC-, PE-, APC-, or biotin (plus avidin PerCP-Cy5.5)-conjugated antibodies; four-color analyses used all of these conjugates, whereas five-color analyses used these conjugates plus APC-Cy7– or Pacific blue–conjugated antibodies. Compensation was done for each fluorochrome to calculate spectral overlap. In parabiotic and adoptive transfer experiments, eGFP or the CD45.1 and CD45.2 alleles were used to identify donor and host-origin cells, and normal mice that were either eGFP$^+$ or eGFP$^-$, or CD45.1$^+$ or CD45.2$^+$ were included as positive and negative fluorescence controls. For multicolor analysis, mixtures of all of the conjugated antibodies minus the relevant antibody were used to determine background fluorescence, as previously described (20). Five million nucleated cells per sample were routinely analyzed to ensure that sufficient DCs were represented (∼10^5 cells in the blood and 5×10^3 cells in the thymus). Results were confirmed by the periodic analysis of DCs enriched on Nycodenz gradients (see the following section). Data were analyzed using FlowJo software (Tree Star, Inc.).

DC isolation and enrichment. Heart blood was collected in heparin and depleted of erythrocytes by treatment with 0.168 M NH_4Cl. Bone marrow cells were obtained by flushing the marrow plugs from the femur and tibia, and dispersing the cells by gentle pipetting. Tissue fragments from the thymus (stripped of attached lymph nodes), lymph nodes, and spleen were digested

for 15 min at 37°C in RPMI 1640 medium with 2% fetal calf serum containing 1 mg/ml collagenase (Sigma-Aldrich) and 0.02 mg/ml DNAase (Boehringer Mannheim) and were mixed in EDTA (5-mM final concentration) for 5 min. No differences in the migratory behavior of the DCs were observed between the enzyme-treated or untreated cell suspensions, but almost twice the number of DCs were recovered after the enzyme treatment. In some experiments, DCs from the cell suspensions were enriched (40–50% purity) by centrifugation in Nycodenz medium (Optiprep 9.5%; Sigma-Aldrich). In other experiments, subsets of DCs were purified (>98%) by sorting on a flow cytometer (Vantage SE; BD).

Purification of monocytes. Monocytes (90–95% purity) were obtained from blood by negative selection on an immunomagnetic column (Miltenyi Biotec). Nucleated cells were labeled with antibodies for MHC II, CD45R, CD43, and CD24 according to the method of Leon et al. (27), treated with MACS anti–rat κ microbeads (20 μl/10^7cells), loaded onto an LS column (500 μl of buffer/10^8 cells), and placed in a magnetic field. The unlabeled fraction (monocyte enriched) was collected in the pass-through fraction, and the labeled fraction (monocyte depleted) was flushed out of the column. The monocyte-enriched fraction was further purified by passage through an MS column. The purity of the monocyte-enriched fraction was then assessed by FACS analysis of light scatter, positive staining for CD11b and F4/80, variable staining (neg/lo or int/hi) for Gr-1, and negative staining for CD11c, CD45R, and MHC II. All other cell types, including granulocytes, were present in the monocyte-depleted fraction.

Adoptive transfer assays for DC migration. In most experiments, normal nonirradiated WT mice were injected in the lateral tail veins with 20×10^6 unfractionated bone marrow, blood, thymus, spleen, or lymph node cells from eGFP tg mice or with proportionate numbers of density gradient–enriched DCs or MACS-enriched monocytes from these tissues. At timed intervals after cell transfer, donor-origin cells (GFP^+) in tissue-cell suspensions were identified, quantified, and phenotyped for surface markers by four- or five-color flow cytometry. In other experiments, 2×10^6 blood cells or proportionate numbers of DCs or monocytes therein were injected intrathymically into the anterior superior portion of each lobe (10 μl per site) using a 1-ml syringe (with attached 28-gauge needle) mounted on a Tridek Stepper (Indicon), as previously described (18, 67). The skin incision was closed with Nexabond Liquid (Veterinary Products). The presence, phenotype, and morphological properties of the donor-origin DCs that appeared in the thymus were examined at timed intervals after i.v. or intrathymic injection.

Parabiosis. Pairs of 4–5-wk-old CD45.1 and CD45.2 congenic mice were surgically joined by cutaneous vascular anastomosis, as previously described (2, 15). The parabiotic mice were maintained for 3 wk before sacrifice or were surgically separated at 3 wk and euthanized 4 wk later. The respective degrees of DC chimerism in the blood and thymus were then determined.

Nested PCR for GFP. Genomic DNA was extracted from tissues and used as templates for nested PCR. Two pairs of PCR primers were used for a single locus within the GFP gene. The first pair of primers, 5′-ATGGTGAGCAAGGGCGAGGAG-3′ (in the 5′ flanking region) and 5′-CTTGTACAGCTCGTCCATGCC-3′ (in the 3′ flanking region), was designed to amplify a fragment within the GFP gene. The second pair of primers, 5′-AGAAGAACGGCATCAAGGTG-3′ (in the 5′ flanking region) and 5′-GAACTCCAGCAGGACCATGT-3′ (in the 3′ flanking region), was used to amplify a fragment within the first PCR product. The amplified PCR products were separated on agarose gel and visualized by ethidium bromide. The sensitivity of the PCR assay was determined by serial dilution of DNA from GFP tg mice and by the use of purposeful mixtures of GFP^+ DCs and GFP^- thymus cells. As few as two mouse cell equivalents of DNA could be detected reliably, as could a ratio of 1 GFP^+ DC mixed with 10^6 GFP^- thymus cells.

In vivo uptake of soluble OVA and fluorescent microspheres. Lyophilized Alexa Fluor 488–conjugated OVA (Invitrogen) was dissolved in endotoxin-free PBS and microcentrifuged to remove aggregates. eGFP tg mice were injected i.v. with 0.5 mg of soluble OVA, and the uptake of OVA by DCs in the blood, spleen, lymph nodes, and thymus was examined by FACS analysis 18 h later. Cells from eGFP tg mice that received buffer only were stained for CD11c, B220, and CD11b and used as controls for background fluorescence in the OVA channel. Parallel experiments using 2-μm Fluoresbrite YG carboxylate microspheres (200 μl of a 2.6% suspension per mouse) and nonfluorescent (control) microspheres (Polysciences) were also conducted.

Cell-cycle analysis. Suspensions of nucleated cells from the blood and thymus were first stained with a panel of antibodies for cell-surface markers. The cells were fixed, permeabilized, and stained for total DNA with 7-AAD using reagents provided in a Flow kit (BD), according to the manufacturer's directions. The proportions of DCs that were in G_0/G_1 or $S/G_2/M$ were determined on individual cells by FACS analysis.

Immunohistology. 10-μm thick serial frozen sections of whole thymus lobes were prepared after the tissue was fixed in 4% paraformaldehyde plus 10% sucrose for 45 min and embedded in optimum cutting temperature medium (Thermo Fisher Scientific). The sections were stained with CD11c-PE antibody or an isotype control for 45 min in a moist chamber and mounted in Vectashield with DAPI (Vector Laboratories). The sections were examined for the intrathymic location of donor (GFP^+) and host-origin (GFP^-) $CD11c^+$ cells by three-color immunofluorescence using a photomicroscope (DP70; Olympus).

We thank Drs. L. Wu and K. Shortman for helpful discussions and suggestions.

This work was supported in part by grants AI49882 and AI060735 from the National Institutes of Health, United States Public Health Service.

The authors have no conflicting financial interests.

Submitted: 6 October 2008
Accepted: 13 February 2009

REFERENCES

1. Wu, L., and K. Shortman. 2005. Heterogeneity of thymic dendritic cells. *Semin. Immunol.* 17:304–312.
2. Donskoy, E., and I. Goldschneider. 2003. Two developmentally distinct populations of dendritic cells inhabit the adult mouse thymus: demonstration by differential importation of hematogenous precursors under steady state conditions. *J. Immunol.* 170:3514–3521.
3. Porritt, H.E., K. Gordon, and H.T. Petrie. 2003. Kinetics of steady-state differentiation and mapping of intrathymic-signaling environments by stem cell transplantation in nonirradiated mice. *J. Exp. Med.* 198:957–962.
4. Wang, Y., I. Goldschneider, D. Foss, D.Y. Wu, J. O'Rourke, and R.E. Cone. 1997. Direct thymic involvement in anterior chamber-associated immune deviation: evidence for a nondeletional mechanism of centrally induced tolerance to extrathymic antigens in adult mice. *J. Immunol.* 158:2150–2155.
5. Wang, Y., I. Goldschneider, J. O'Rourke, and R.E. Cone. 2001. Blood mononuclear cells induce regulatory NK T thymocytes in anterior chamber-associated immune deviation. *J. Leukoc. Biol.* 69:741–746.
6. Wu, D.Y., and I. Goldschneider. 1999. Cyclosporine A-induced autologous graft-versus-host disease: a prototypical model of autoimmunity and active (dominant) tolerance coordinately induced by recent thymic emigrants. *J. Immunol.* 162:6926–6933.
7. Wu, D.Y., and I. Goldschneider. 2001. Tolerance to cyclosporine A-induced autologous graft-versus-host disease is mediated by a CD4+CD25+ subset of recent thymic emigrants. *J. Immunol.* 166:7158–7164.
8. Beschorner, W.E., X. Yao, and J. Divic. 1995. Recruitment of semi-allogeneic dendritic cells to the thymus during post-cyclosporine thymic regeneration. *Transplantation.* 60:1326–1330.
9. Derbinski, J., J. Gabler, B. Benedikt, S. Tierling, S. Jonnakuty, M. Hergenhahn, L. Peltonen, J. Walter, and B. Kyewski. 2005. Promiscuous gene expression in thymic epithelial cells is regulated at multiple levels. *J. Exp. Med.* 202:33–45.

10. Goldschneider, I., and R.E. Cone. 2003. A central role for peripheral dendritic cells in the induction of acquired thymic tolerance. *Trends Immunol.* 24:77–81.
11. Proietto, A.I., S. van Dommelen, P. Zhou, A. Rizzitelli, A. D'Amico, R.J. Steptoe, S.H. Naik, M.H. Lahoud, Y. Liu, P. Zheng, K. Shortman, and L. Wu. 2008. Dendritic cells in the thymus contribute to T regulatory cell induction. *Proc. Natl. Acad. Sci. USA.* 105:19869–19874.
12. Colonna, M., G. Trinchieri, and Y.J. Liu. 2004. Plasmacytoid dendritic cells in immunity. *Nat. Immunol.* 5:1219–1226.
13. Moseman, E.A., X. Liang, A.J. Dawson, A. Panoskaltsis-Mortari, A.M. Krieg, Y.J. Liu, B.R. Blazer, and W. Chen. 2004. Human plasmacytoid dendritic cells activated by CpG oligodeoxynucleotides induce the generation of CD4+CD25+ regulatory T cells. *J. Immunol.* 173:4433–4442.
14. Martin, P., G. Martina del Hoyo, F. Anjuere, C. Arias, H. Vargas, V. Parrillas, and C. Ardavin. 2002. Characterization of a new subpopulation of mouse CD8α^+ B220$^+$ dendritic cells endowed with type 1 interferon production capacity and tolerogenic potential. *Blood.* 100:383–390.
15. Donskoy, E., and I. Goldschneider. 1992. Thymocytopoiesis is maintained by blood-borne precursors throughout postnatal life. A study in parabiotic mice. *J. Immunol.* 148:1604–1612.
16. Naik, S.H., L.M. Corcoran, and L. Wu. 2005. Development of murine plasmacytoid dendritic cell subsets. *Immunol. Cell Biol.* 83:563–570.
17. Okada, T., Z. Lian, M. Naiki, N. Mitsuri, A. Ansari, S. Ikehara, and M. Gershwin. 2003. Murine thymic plasmacytoid dendritic cells. *Eur. J. Immunol.* 33:1012–1019.
18. Foss, D.L., E. Donskoy, and I. Goldschneider. 2001. The importation of hematogenous precursors by the thymus is a gated phenomenon in normal adult mice. *J. Exp. Med.* 193:365–374.
19. Duncan, S.R., N.G. Capetanakis, B.R. Lawson, and A.N. Theofilopoulos. 2002. Thymic dendritic cells traffic to thymi of allogeneic recipients and prolong graft survival. *J. Clin. Invest.* 109:755–764.
20. O'Keeffe, M.O., H. Hubertus, D. Vermec, I. Caminschi, J.L. Miller, E.M. Anders, L. Wu, M.H. Lahoud, S. Henri, B. Scott, et al. 2002. Mouse plasmacytoid cells: long-lived cells, heterogeneous in surface phenotype and function, that differentiate into CD8$^+$ dendritic cells only after microbial stimulus. *J. Exp. Med.* 196:1307–1319.
21. Diao, J., E. Winter, W. Chen, C. Cantin, and M. Cattral. 2004. Characterization of distinct conventional and plasmacytoid dendritic cell-committed precursors in murine bone marrow. *J. Immunol.* 173:1826–1833.
22. Latour, S., H. Tanaka, C. Demeure, V. Mateo, M. Rubio, E.J. Brown, C. Maliszewski, F.P. Lindberg, A. Oldenborg, A. Ullrich, et al. 2001. Bidirectional negative regulation of human T and dendritic cells by CD47 and its cognate receptor signal-regulator protein-α: down-regulation of IL-12 responsiveness and inhibition of dendritic cell activation. *J. Immunol.* 167:2547–2554.
23. Randolph, G.J., S. Bealieu, S. Lebecque, R. Steinman, and W. Muller. 1998. Differentiation of monocytes into dendritic cells in a model of transendothelial trafficking. *Science.* 282:480–483.
24. Randolph, G.J., K. Inaba, D. Robbiani, R. Steinman, and W. Muller. 1999. Differentiation of phagocytic monocytes into lymph node dendritic cells in vivo. *Immunity.* 11:753–761.
25. Leon, B., M. Lopez-Bravo, and C. Ardavin. 2007. Monocyte-derived dendritic cells formed at the infection site control the induction of protective T helper responses against *Leishmania*. *Immunity.* 26:519–531.
26. Shortman, K., and S. Naik. 2007. Steady-state and inflammatory dendritic-cell development. *Nat. Rev. Immunol.* 7:19–30.
27. Leon, B., G. Martinez del Hoyo, V. Parrillas, H. Hernandez Vargas, P. Sanchez-Mateos, N. Longo, M. Lopez-Bravo, and C. Ardavin. 2004. Dendritic cell differentiation potential of mouse monocytes: monocytes represent immediate precursors of CD8$^-$ and CD8$^+$ splenic dendritic cells. *Blood.* 103:2668–2676.
28. Diao, J., E. Winter, C. Cantin, W. Chen, L. Xu, D. Kelvin, J. Phillips, and M. Cattral. 2006. In situ replication of immediate dendritic cell (DC) precursors contributes to conventional DC homeostasis in lymphoid tissue. *J. Immunol.* 176:7196–7206.
29. Naik, S.H., D. Metcalf, A. van Nieuwenhuijze, I. Wicks, L. Wu, M. O'Keefe, and K. Shortman. 2006. Intrasplenic steady-state dendritic cell precursors that are distinct from monocytes. *Nat. Immunol.* 7:663–671.
30. Geissmann, F., S. Jung, and D.R. Littman. 2003. Blood monocytes consist of two principal subsets with distinct migratory properties. *Immunity.* 19:71–82.
31. Prockop, S.E., and H.T. Petrie. 2004. Regulation of thymus size by competition for stromal niches among early T cell progenitors. *J. Immunol.* 173:1604–1611.
32. Rodewald, H.R., T. Brocker, and C. Haller. 1999. Developmental dissociation of thymic dendritic cell and thymocyte lineages revealed in growth factor receptor mutant mice. *Proc. Natl. Acad. Sci. USA.* 96:15068–15073.
33. Vandenabeele, S., H. Hochrein, N. Mavaddat, K. Winkel, and K. Shortman. 2001. Human thymus contains 2 distinct dendritic-cell populations. *Blood.* 97:1733–1741.
34. Vremec, D., J. Pooley, H. Hochrein, L. Wu, and K. Shortman. 2000. CD4 and CD8 expression by dendritic cell subtypes in mouse thymus and spleen. *J. Immunol.* 164:2978–2986.
35. Ferrero, I., W. Held, A. Wilson, F. Tacchini-Cottier, F. Radtke, and H.R. MacDonald. 2002. Mouse CD11c$^+$ B220$^+$ Gr1$^+$ plasmacytoid dendritic cells develop independently of the T-cell lineage. *Blood.* 100:2852–2857.
36. Takeuchi, S., and S. Katz. 2006. Use of interleukin 7 receptor-alpha knockout donor cells demonstrates the lymphoid independence of dendritic cells. *Blood.* 107:184–186.
37. Weijer, K., C. Uittenbogaart, A. Voordouw, F. Couwenberg, J. Seppen, B. Blom, F. Vyth-Dreese, and H. Spits. 2002. Intrathymic and extrathymic development of human plasmacytoid dendritic cell precursors in vivo. *Blood.* 99:2752–2759.
38. Ito, T., M. Yang, Y. Wang, R. Lande, J. Gregorio, O. Perng, X. Qin, Y. Liu, and M. Gilliet. 2007. Plasmacytoid dendritic cells prime IL-10–producing T regulatory cells by inducible costimulator ligand. *J. Exp. Med.* 204:105–115.
39. Saunders, D., K. Lucas, J. Ismaili, L. Wu, E. Maraskovsky, A. Dunn, and K. Shortman. 1996. Dendritic cell development in culture from thymic precursor cells in the absence of granulocyte/macrophage colony-stimulating factor. *J. Exp. Med.* 184:2185–2196.
40. Bonasio, R., M.L. Scimone, P. Schaerli, N. Grabie, A.H. Lichtman, and U.H. von Andriam. 2006. Clonal deletion of thymocytes by circulating dendritic cells homing to the thymus. *Nat. Immunol.* 7:1092–1100.
41. Liu, K., C. Waskow, X. Liu, K. Yao, J. Hoh, and M. Nussenzweig. 2007. Origin of dendritic cells in peripheral lymphoid organs of mice. *Nat. Immunol.* 8:578–583.
42. de Vries, H.E., J.J. Hendriks, H. Honing, C. Renardel de Lavalette, S.M.A. van der Pol, E. Hooijberg, C.D. Dijkstra, and T.K. van den Berg. 2002. Signal-regulatory protein alpha-CD47 interactions are required for the transmigration of monocytes across cerebral endothelium. *J. Immunol.* 168:5832–5839.
43. Liu, Y., H.J. Buhring, K. Zen, S.L. Burst, F.J. Schnell, I.R. Williams, and C.A. Parkos. 2002. Signal regulatory protein (SIRP alpha) a cellular ligand for CD47, regulates neutrophil transmigration. *J. Biol. Chem.* 277:10028–10036.
44. Garrod, K.R., C.K. Chang, F.C. Liu, T.V. Brennan, R.D. Foster, and S.M. Kang. 2006. Targeted lymphoid homing of dendritic cells is required for prolongation of allograft survival. *J. Immunol.* 177:863–868.
45. Hintzen, G., L. Ohl, M.L. del Rio, J.I. Barbosa-Rodriquez, O. Pabst, J.R. Kocks, J. Krege, S. Hardtke, and R. Forster. 2006. Induction of tolerance to innocuous inhaled antigen relies on a CCR7-dependent dendritic cell-mediated antigen transport to the bronchial lymph node. *J. Immunol.* 177:7346–7345.
46. Braun, D., L. Galibert, T. Nakajima, H. Saito, V. Quang, M. Rubio, and M. Sarfati. 2006. Semimature stage: a checkpoint in a dendritic cell maturation program that allows for functional reversion after signal-regulatory protein-alpha ligation and maturation signals. *J. Immunol.* 177:8550–8559.
47. Watanabe, N., Y.H. Wang, H.K. Lee, T. Ito, Y.H. Wang, W. Cao, and Y.J. Liu. 2005. Hassall's corpuscles instruct dendritic cells to induce CD4$^+$CD25$^+$ regulatory T cells in human thymus. *Nature.* 436:1181–1185.
48. Proietto, A.I., M.H. Lahoud, and L. Wu. 2008. Distinct functional capacities of mouse thymic and splenic dendritic cell populations. *Immunol. Cell Biol.* 86:700–708.
49. Lan, Y.Y., Z. Wang, G. Raimondi, W. Wu, B.L. Colvin, A.D. Creus, and A.W. Thomson. 2006. "Alternatively activated" dendritic cells

preferentially secrete IL-10, expand Foxp3$^+$CD4$^+$ T cells, and induce long-term organ allograft survival in combination with CTLA4-Ig. *J. Immunol.* 177:5868–5877.
50. Marschner, A., S. Rothenfusser, V. Hornung, D. Prell, A. Krug, M. Kerkmann, D. Wellisch, H. Poeck, A. Greinacher, T. Giese, et al. 2005. CpG ODN enhance antigen-specific NKT cell activation via plasmacytoid dendritic cells. *Eur. J. Immunol.* 35:2347–2357.
51. Ochando, J.C., C. Homma, Y. Yang, A. Hidalgo, A. Garin, F. Tacke, V. Angeli, Y. Li, P. Boros, Y. Ding, et al. 2006. Alloantigen-presenting plasmacytoid dendritic cells mediate tolerance to vascularized grafts. *Nat. Immunol.* 7:652–662.
52. Khoury, S.J., L. Gallon, W. Chen, K. Betres, M.E. Russell, W.W. Hancock, C.B. Carpenter, M.H. Sayegh, and H.L. Weiner. 1995. Mechanisms of acquired thymic tolerance in experimental autoimmune encephalomyelitis: thymic dendritic-enriched cells induce specific peripheral T cell unresponsiveness in vivo. *J. Exp. Med.* 182:357–366.
53. Sayegh, M.H., N. Perico, O. Imberti, W.W. Hancock, C.B. Carpenter, and G. Remuzzi. 1993. Thymic recognition of class II major histocompatibility complex allopeptides induces donor-specific unresponsiveness to renal allografts. *Transplantation.* 56:461–465.
54. Hackstein, H., E. Morelli, and A.W. Thomson. 2001. Designer dendritic cells for tolerance induction: guided not misguided missiles. *Trends Immunol.* 22:437–442.
55. Young, K.J., L. Yang, M.J. Phillips, and L. Zhang. 2002. Donor-lymphocyte infusion induces transplantation tolerance by activating systemic and graft-infiltrating double-negative regulatory T cells. *Blood.* 100:3408–3418.
56. Deng, S., D.J. Moore, X. Huang, M. Mohiuddin, M.K. Lee IV, E. Velidedeoglu, M.-M. Lian, M. Chiaccio, S. Sonawane, A. Orlin, et al. 2006. Antibody-induced transplantation tolerance that is dependent on thymus-derived regulatory T cells. *J. Immunol.* 176:2799–2807.
57. Chiffoleau, E., G. Bériou, P. Dutartre, C. Usal, J.-P. Soulillou, and M.C. Cuturi. 2002. Role for thymic and splenic regulatory CD4$^+$ T cells induced by donor dendritic cells in allograft tolerance by LF15-0195 treatment. *J. Immunol.* 168:5058–5069.
58. Huseby, E.S., B. Sather, P.G. Huseby, and J. Goverman. 2001. Age-dependent T cell tolerance and autoimmunity to myelin basic protein. *Immunity.* 14:471–481.
59. Garrovillo, M., A. Ali, H. Depaz, R. Gopinathan, O.O. Oluwole, M.A. Hardy, and S.E. Oluwole. 2001. Induction of transplant tolerance with immunodomiant allopeptide-pulsed host lymphoid and myeloid dendritic cells. *Am. J. Transplant.* 1:129–137.
60. Huang, F.P., N. Platt, M. Wykes, J.R. Major, T.J. Powell, C.D. Jenkins, and G.G. MacPherson. 2000. A discrete subpopulation of dendritic cells transports apoptotic intestinal epithelial cells to T cell areas of mesenteric lymph nodes. *J. Exp. Med.* 191:435–444.
61. Bonasio, R., and U.H. von Andrian. 2006. Generation, migration and function of circulating dendritic cells. *Curr. Opin. Immunol.* 18:503–511.
62. Tada, K., M. Tanaka, R. Hanayama, K. Miwa, A.I. Shinohara, and S. Nagata. 2003. Tethering of apoptotic cells to phagocytes through binding of CD47 to Src homology 2 domain-bearing protein tyrosine phosphatase substrate-1. *J. Immunol.* 171:5718–5726.
63. Pacholczyk, R., J. Kern, N. Singh, M. Iwashima, P. Kraj, and L. Ignatowicz. 2007. Nonself-antigens are the cognate specificities of Foxp3$^+$ regulatory T cells. *Immunity.* 27:493–504.
64. Belkaid, Y. 2007. Regulatory T cells and infection: a dangerous necessity. *Nat. Rev. Immunol.* 7:875–888.
65. Sehrawat, S., S. Suvas, P. Sarangi, A. Suryawanshi, and B. Rouse. 2008. In vitro-generated antigen-specific CD4+ CD25+ Foxp3+ regulatory T cells control the severity of herpes simplex virus-induced ocular immunoinflammatory lesions. *J. Virol.* 82:6838–6851.
66. Durkin, H.G., S. Chice, and I. Goldschneider. 1984. Origin and fate of antigen-specific suppressor T cells. *Ann. NY Acad. Sci.* 435:258–259.
67. Goldschneider, I., K. Komschilies, and D. Greiner. 1986. Studies of thymocytopoiesis in rats and mice. I. Kinetics of appearance of thymocytes using a direct intrathymic adoptive transfer assay for thymocyte precursors. *J. Exp. Med.* 163:1–17.